

Analysis of Cassegrain Cloud Profiling Radar Antenna With Arbitrary Projected Apertures¹

Ziad A. Hussein and Eastwood Im
Jet Propulsion Laboratory
California Institute of Technology
4800 Oak Grove Dr.
Pasadena, California 91109
818-354-0533
ziad.a.hussein@jpl.nasa.gov

Abstract—A millimeter wave Cassegrain dual-reflector radar antenna (~94GHz) with super-quadric projected aperture boundaries concept, that includes sub-reflector blockage effect, is evaluated for the spaceborne radar measurement of the vertical cloud profile structure. In this paper, we show how the super-quadric aperture representation may be used for optimizing the antenna radiation performance. This yields to reduce the noise/clutter level received by the radar through the antenna. In particular, where the design specifications stipulate desired radiation characteristics (gain, sidelobe levels and beamwidths) and maximum allowable antenna dimensions for nadir looking beam. Model results based on physical optics, PO, and uniform theory of diffraction, UTD, for different projected apertures *super-quadric boundaries* show that the trends of the antenna patterns in the principal planes differ significantly from those in the ± 45 degrees planes. These unique characteristics along with the pronounce impact of the edge tapers on the first sidelobe level relative to the adjacent ones provide a basis to obtain an optimum antenna design for the instrument.

TABLE OF CONTENTS

1. INTRODUCTION
2. ANTENNA ANALYSIS
3. ANTENNA OPTIMIZATION
4. SUMMARY

1. INTRODUCTION

A millimeter wave Cassegrain dual-reflector antenna (~94 GHz) with super-quadric aperture boundaries concept is evaluated for the spaceborne cloud profiling radars. The instrument is designed to measure profiles of cloud water and ice in the atmosphere in combinations with optical depths using a nadir looking beam. The principle operation of the cloud radar is to transmit pulses and measure the backscattered power of the cloud layers versus time. Hence,

this process provides the cloud reflectivity data versus altitude. However, the data received may be contaminated by surface clutter. For a nadir pointed antenna the primary source of noise/clutter for the instrument is the surface backscatter return from previous pulses transmitted and received through the antenna sidelobes. Consequently, particularly challenging in the specifications for the antenna requirements are the unique very low sidelobes levels desired at far-angle from the peak of the beam. The antenna proposed for the instrument is a Cassegrain dual-reflector, shown in Figure 1, that consists of a parabolic main reflector with super-quadric projected aperture, and a hyperboloid sub-reflector illuminated by a pyramidal feed horn. The design specifications stipulate desired radiation characteristics (gain ~ 63 dB, first sidelobe level ~ 15 dB and far-sidelobe level ~ 40 dB below main beam peak, and beamwidths ~0.11 degrees) and maximum allowable antenna dimension (~1.85 m). It is imperative that a very accurate and real life antenna model (that includes the sub-reflector blockage effects) is developed. This step is necessary in order to be able to obtain an optimum antenna design and effectively assess and characterize its RF performance, and critically investigate the key parameters that yield optimum antenna gain and far sidelobe levels reduction.

2. ANTENNA ANALYSIS

Diffraction analysis procedures based on PO/UTD [1]-[3] for different projected aperture *super-quadric boundary* [4] are implemented to determine its impact on side-lobe level reduction and gain. The formulation is accomplished by representing the projected aperture boundary in the x - y plane as a super-quadric curve (see Figure 2):

$$\left| \frac{x}{a} \right|^n + \left| \frac{y}{b} \right|^n = 1 \quad (1)$$

¹ 0-7803-5846-5/00/\$10.00 ©2000 IEEE

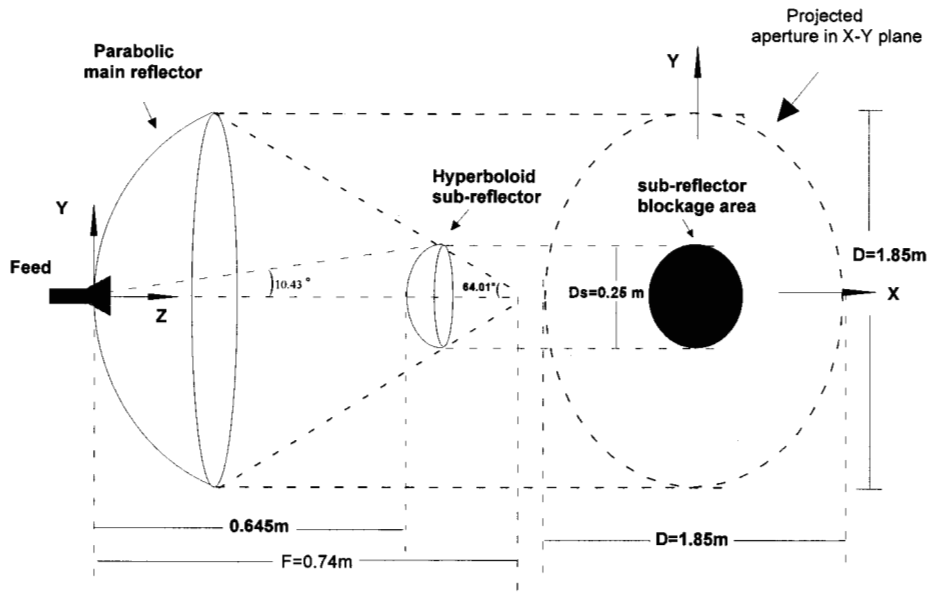


Figure 1. Cloud-SAT 94.1 GHz Cassegrain Dual -Reflector Cloud Profiling Radar Antenna ($f/D=0.4$, antenna diameter, $D=1.85\text{m}$, and sub-reflector diameter $D_s=0.25\text{ m}$)

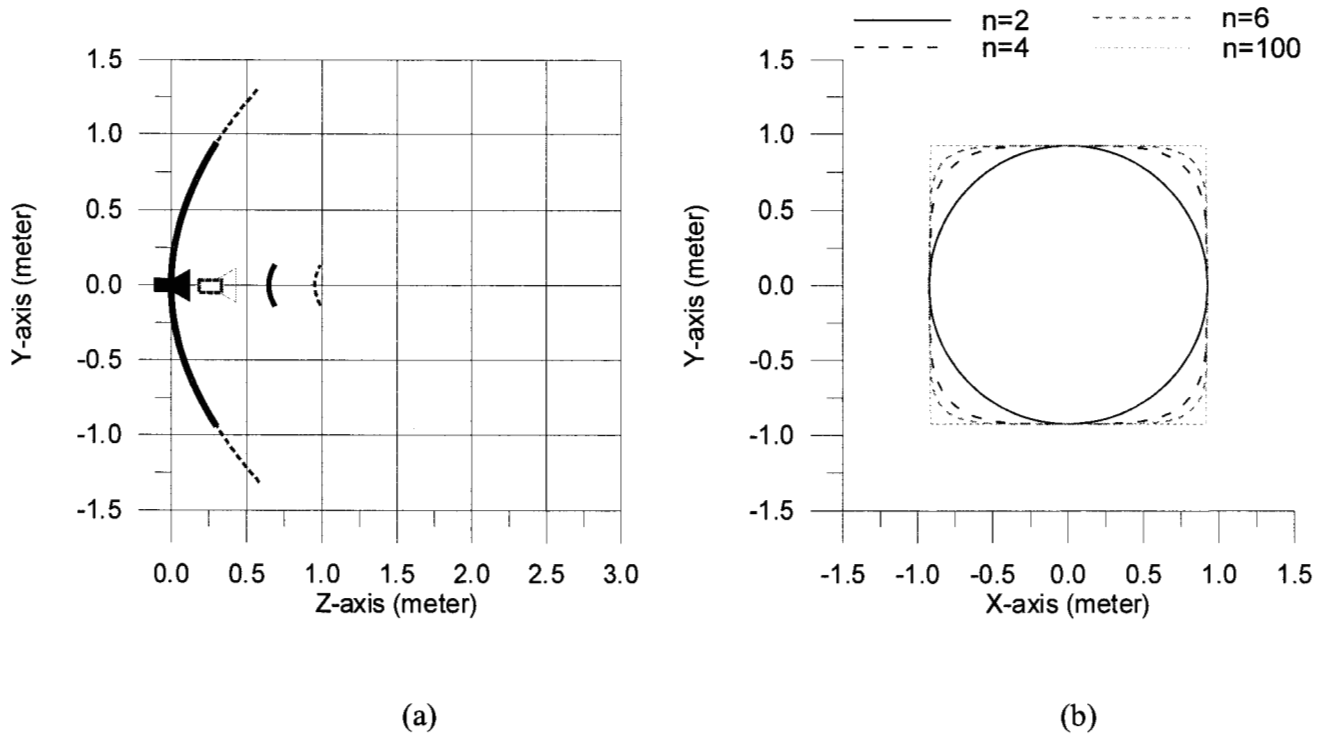


Figure 2. (a) Surface Profiles For Two Cassegrain Dual-Reflector Antennas With The Same F/D Ratio (Solid And Dotted Lines Correspond To $D=1.85\text{m}$ and $D=2.6163\text{m}$, Respectively). (b) Cassegrain Dual-Reflector Super-Quadric projected Apertures In X-Y Plane for different values of n .

where a , b are the semi-axes in the x and y direction respectively, and n is the parameter that provides the capability to control the shape of the curvature corners as shown in Figure 2b. It is evident from equation (1) that the super-quadric representation allows modeling of numerous different projected aperture curve configurations through variation of the parameters, a , b , and n . Figure 2b illustrates the effect of various values of n on the curve geometry for the proposed antenna design with an aspect ratio of $b/a=1$.

3. ANTENNA OPTIMIZATION

In view of the key issues described above, our optimization approach is based on two steps. In the first, we used a circular projected aperture to define the antenna baseline design. In step two, we used a super-quadric projected aperture to optimize the antenna performance:

1) Circular Aperture

The first step deals with obtaining the antenna performance using PO/UTD [1]-[5], for a circular projected aperture (1.85-meter in diameter), and a focal to diameter ratio, f/D , of 0.4 as to keep the antenna assembly compact. In this analysis, we included the sub-reflector blockage effect. That is, it is assumed that the PO currents on the main reflector that fall within the geometrical optics shadow of the sub-reflector, when the latter is illuminated by far-source, don't radiate. This entails zeroes the PO currents in the shadow region. For optimum antenna gain, a -10 dB edge taper, ET, is used. This corresponds to a feed pattern with a cosine to the power, q , equal to 68.6 (the feed is located at the apex of the parabolic reflector as shown in Figure 1).

Next, we implemented an equivalent field model for a millimeter wave feed horn to determine whether a physically realizable feed horn (to illuminate the sub-reflector) can be designed such that its radiation patterns match the desired $\cos^{68.6}(\theta)$ feed pattern. The $\cos^q(\theta)$ feed pattern is used as an input to the PO/UTD analysis. Consequently, the resulting feed-horn patterns can be used in the analysis to obtain far-accurate representation of the antenna performance.

This model is based on the application of the Equivalence Principle, in which the horn's aperture fields are replaced by equivalent magnetic and electric currents in the aperture. The aperture field is assumed to have a TE_{10} amplitude distribution, and quadratic phase variation depending upon the length and flares angles of the horn. This method provides accurate far field patterns for angular regions near the main lobe and its closet minor lobes. Noteworthy, a standard WR-10 waveguide is incorporated into the formulation to connect to the pyramidal sectoral flares as shown in Figure 3. The WR-10 waveguide supports the

TE_{10} dominant mode between 75-110 GHz. The radiation pattern cuts in E-, H-, and 45° planes of the feed horn design are computed and compared to the desired $\cos^{68.6}(\theta)$ patterns as shown in Figure 4. As can be seen that the patterns have excellent agreement over the angular region $\pm 10.43^\circ$ illuminating the sub-reflector. The horn dimensions related to these patterns are computed, and found to be physically realizable. Figure 3 shows the physically realizable pyramidal feed horn front view dimensions. The calculated horn directivity, and 3-dB beamwidth are 23.35 dB and 11.6° respectively.

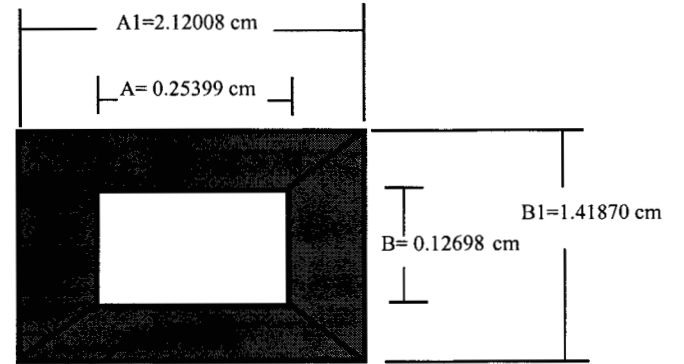


Figure 3. Front view of the millimeter wave feed horn design for the 94.1 GHz Cassegrain dual reflector

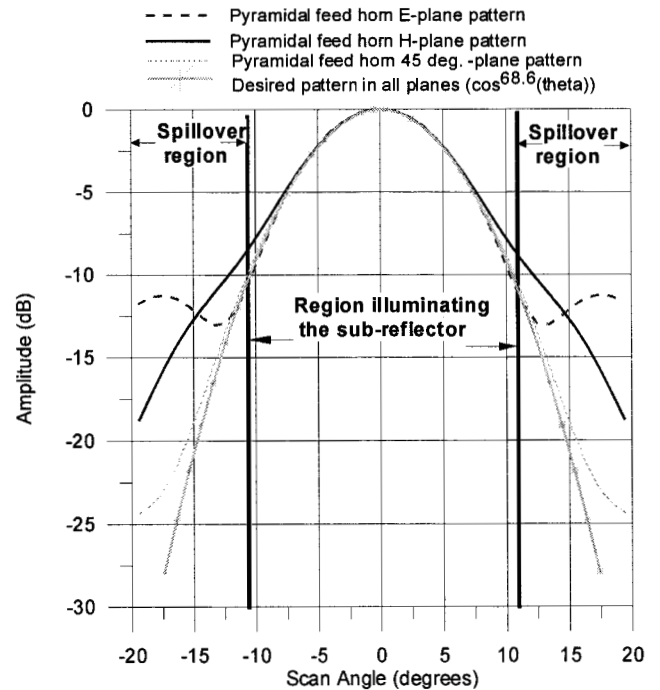


Figure 4. Comparison between the $\cos^q(\theta)$ desired feed horn patterns ($q=68.6$) and the 94.1 GHz pyramidal horn E-, H-, and 45° plane patterns.

Performance Characterizations:

A comparison between antenna patterns with and without central blockage effect for a -10 dB, and -20 dB edge taper, illumination are shown in Figure 5a and b respectively. The PO/UTD blockage/shadowing results predict the loss in gain to be approximately 0.42 dB (ET=-10 dB). The peak of the first sidelobe level increases approximately 4 dB. Critical to the Cassegrain antenna design, in which very low sidelobe levels are desired, is the relationship between tapered feed illumination, antenna gain, and beamwidth. Table 1. contains all the results of this analysis. In performing this analysis, the edge taper was varied and the resulting antenna gain, beamwidth, and radiation pattern computed. Results are shown for edge tapered of -20dB, -15dB, and -10dB for the antenna configuration shown in Figure 1. As one would expect, the maximum gain is achieved for approximately a -10dB edge taper. However, the antenna far sidelobe levels remains relatively the same for a broad range of edge taper -10 to -20 dB, with the exception of the first sidelobe level closer to the peak of the beam as shown in Figure 5a and b. The first sidelobe level is reduced by approximately 5 dB for edge taper range -10 to -20dB. Also note that large feed edge taper, i.e. ET=-20 dB, results in null-filling and broadening the sidelobe beamwidth as shown in Figure 5b.

Table 1. Antenna gain and beamwidth results with sub-reflector central blockage/shadowing effect for different feed edge tapered illumination

| ET (dB) | Gain (dB) | Beamwidth (degrees) |
|---------|-----------|---------------------|
| -10 | 63.90 | 0.112 |
| -15 | 63.70 | 0.118 |
| -20 | 63.20 | 0.126 |

Similar observations were made in the extensive theoretical and experimental work on the feed-support plate blockage effect on the antenna pattern and gain for the SeaWinds dual-beam reflector antenna [6].

For the spaceborne cloud profiling radars, it is anticipated that the noise effect of the first sidelobe level on contaminating the radar cross section data may be reduced during radar data processing. Therefore, one can select the illumination edge taper (ET=-10dB) for desired maximum gain, since high feed edge taper doesn't lend itself for far-sidelobe level reduction as the general notion indicates without the central blockage/shadowing effect.

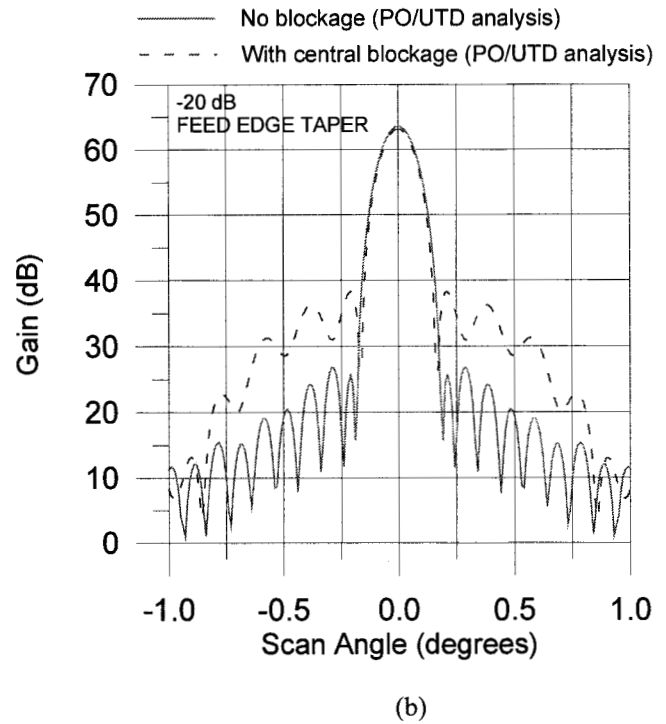
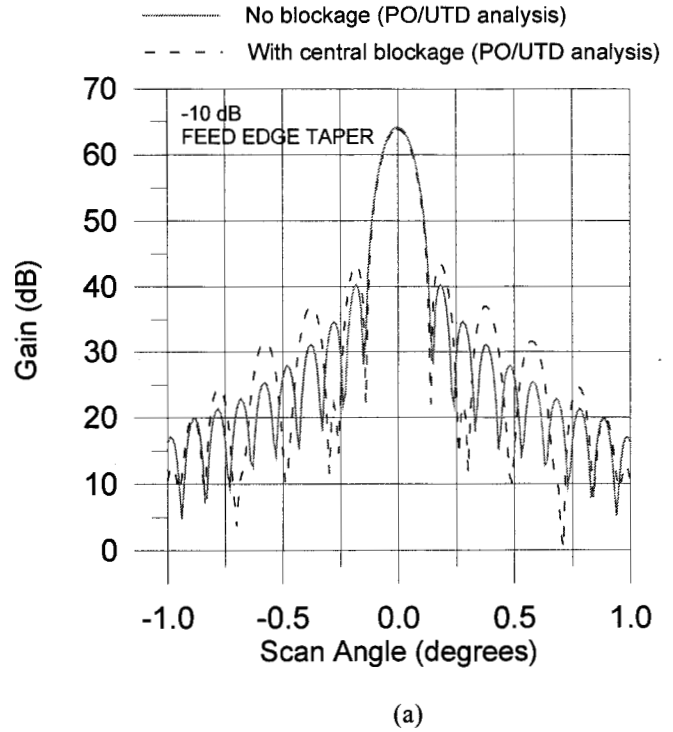


Figure 5. PO/UTD Analysis Results With And Without Central Blockage Effect For A 94.1 GHz Cassegrain Dual-Reflector For The Design Configuration In Figure 1. (a) -10 dB Tapered Feed Illumination, (b) -20 dB Tapered Feed Illumination.

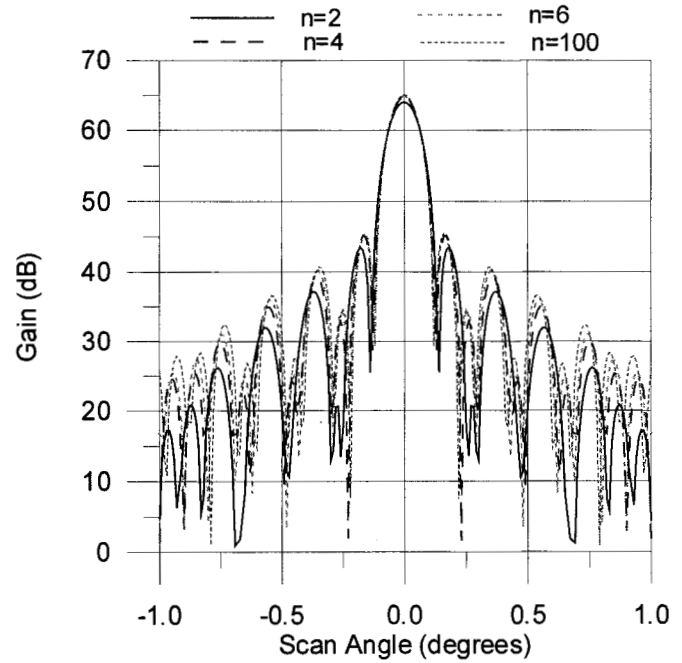
2) Super-Quadric Projected Apertures

Our objective here is to optimize the antenna performance (1.85m diameter) described in step 1. Our initial approach is based on using larger aperture diameter (e.g. 2.6163 m) with the same f/D ratio as in step 1. Figure 2a describes the main reflector profiles in y-z plane, and the corresponding new feed and sub-reflector locations. The main reflector is under-illuminated such that the inner portion of it (1.85 m) is illuminated with -10 dB edge taper (similar illumination as in step 1). A super-quadric aperture with diameter of 1.85 meter is superimposed on the antenna-projected aperture as shown in Figure 2b. Physical optics currents are set to zero for points located on the reflector and correspond to points outside the super-quadric aperture. In this case and for n equal to 2, one can obtain the antenna performance parameters as in step 1. As can be seen from Figure 6 that the trends of the antenna patterns in the principal planes (Figure 6a) differ significantly from those in the ± 45 degrees planes (Figure 6b) for values of n greater than 2. As expected, for larger values of n , higher antenna gain (see Table 2. below) and lower sidelobes levels are obtained in any planes other than the principal planes as shown in Figure 6b.

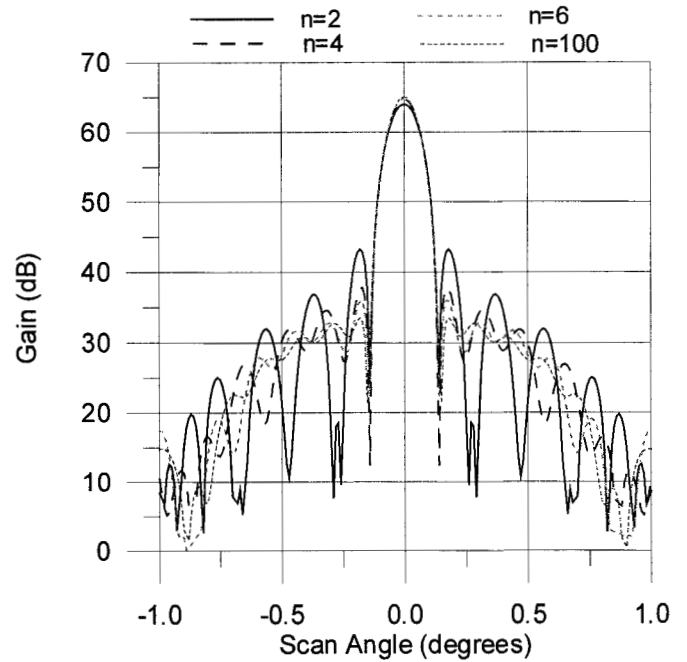
Table 2. Antenna gain for various values of n and for $a=b=D/2$ ($D=1.85$ m)

| n | Gain (dB) |
|-----|-----------|
| 2 | 64.00 |
| 4 | 64.70 |
| 6 | 64.88 |
| 100 | 65.05 |

Hence, the overall noise clutter received by the antenna sidelobes (in 3-D space) may be reduced by using super-quadric projected apertures (e.g., $n=4, 6$). It should be noted here that the loss of antenna gain due to the use of high edge taper (e.g., -20 dB) can be compensated for with the use of super-quadric aperture (e.g., $n=4, 6$). While the benefit of the use of high taper as described in step 1 is pronounced on the first sidelobe level reduction in the antenna patterns -including the principal planes, the use of super-quadric aperture results in reduction of sidelobes levels in planes other than the principals. Hence, the use of super-quadric aperture together with appropriate edge taper leads to optimize the antenna performance, and consequently reduced the noise/clutter received by the instrument.



(a)



(b)

Figure 6. Far-Field Radiation Patterns For Different Super-Quadric Projected Aperture Boundaries, n . (a) Principal Plane $\phi=0$ or Y-Z, (b) $\phi=45$ degrees Plane

4. SUMMARY

A study has been performed for the utility of a super-quadric projected aperture of a Cassegrain dual-reflector with application to cloud profile structure measurements. It is been shown that the use of super-quadric projected aperture is advantageous in reducing the noise/clutter level received by the instrument through the antenna sidelobes. The appropriate use of edge taper together with super-quadric projected aperture (e.g., $n=4, 6$) ultimately yield to optimize the antenna design performance.

ACKNOWLEDGMENTS

The research described in this paper was performed by the Jet Propulsion Laboratory, California Institute of Technology, under contract with the National Aeronautics and Space Administration.

REFERENCES

- [1] O. M. Bucci, G. Franceschetti and G. D'Ella , "Fast Analysis of Large Antennas- A New Computational Philosophy" IEEE Transactions on Antennas and Propagation, Vol. Ap-28, No. 3, pp 306-310, May 1980.
- [2] P.T. Lam, S. W. Lee, C.C. Hung, and R. Acosta "Strategy for Reflector Pattern Calculation: Let The Computer Do the Work", IEEE Transactions on Antennas and Propagation, Vol. Ap-34, No. 3, pp 593-597, April 1986.
- [3] D. Duan and Y. Rahmat-Samii, "A generalized Diffraction synthesis technique for high performance reflector antennas" *IEEE Transaction on Antennas and Propagation*. Jan. 1995.
- [4] Z. A. Hussein, and E. Im "On The Scan Performance of Phased Array Fed Cylindrical Reflector With Super Quadric Projected Aperture: PO/FFT Analysis" The Journee Internationales de Nice sur les Antennes (JINA 98), Nice, France, pp. 386-389, November 1998.
- [5] O. M. Bucci, G. Franceschetti, "Radiation from Reflector Antennas: Exact Aperture and Aperture-Like Approaches", *Radio Science*, Vol 16, No. 6, pp 1101-1104, Nov-Dec 1981.
- [6] Z. A. Hussein, Y. Rahmat-Samii, and K. Kellogg, "Design And Near-Field Measurement Performance Evaluation of The SeaWinds Dual-Beam Reflector Antenna" 1997 IEEE Antennas And Propagation Int. Symp., and URSI North American Radio Science Meeting, Montreal, Canada, pp. 852-855, July 1997.

Ziad A. Hussein received the BSEE from the University of Massachusetts at Amherst, and the MSEE degree in 1991. He is currently working toward the Ph.D degree at UCLA. He has been a member of Technical staff at JPL since 1991 and has made fundamental contribution to the design, analysis and cylindrical near-field calibration of the NASA Scatterometer (NSCAT) and SeaWinds Spaceborne Scatterometer instruments (he was the Cognizant Engineer for the SeaWinds radar antenna and the Cognizant Engineer for near-field radar antenna calibration). He has developed a number of algorithms for near-field data processing, microwave imaging in cylindrical and planar near-field scanning, and antennas. He has been actively involved in several spaceborne antennas research for LightSAR, Cloud-SAT, and other Earth science missions. He is also involved with the in-situ advanced radar sounder research for Mars Outpost Site Survey. He is the recipient of the NASA certificate of recognitions.

Eastwood Im is the Supervisor of the Radar Science Applications Group at JPL, and the Radar Instrument Manager of the ESSP CloudSat Mission. He has extensive experience in spaceborne meteorological radar science and remote sensing, and advanced radar system studies. Dr. Im is the Principal Investigator of the TRMM radar calibration study and a member of the TRMM Radar Science Team, and the Principal Investigator of the NASA IIP Second-Generation Precipitation Radar (PR-2) task. He has been a member of Science Steering Group for the EOS-9 Global Precipitation Mission since the start of the planning phase. Dr. Im is currently the Associate Editor of the AMS Journal of Atmospheric and Oceanic Technology. He has over 80 refereed journal and conference publications.